Pharm Res (2012) 29:2017–2029
DOI 10.1007/s11095-012-0729-1

RESEARCH PAPER

Enhanced Topical Delivery of Small Hydrophilic or Lipophilic Active Agents and Epidermal Growth Factor by Fractional Radiofrequency Microporation

Jaekwan Kim • Ji-Hye Jang • Ji Hae Lee • Jin Kyu Choi • Woo-Ram Park • Il-Hong Bae • Joonho Bae • Jin Woo Park

Received: 8 January 2012 / Accepted: 29 February 2012 / Published online: 8 March 2012

ABSTRACT

Purpose To evaluate the ability of a novel radiofrequency (RF) microporation technology based on ablation of the skin barrier to enhance topical delivery of active ingredients

Methods The influence of RF fluence and the molecular size of the absorbent on the permeation enhancement was confirmed by *in vitro* skin permeation study using Franz diffusion cells. The improved skin rejuvenation effects, such as depigmentation and anti-wrinkle effects, by enhanced topical delivery of α-bisabolol and epidermal growth factor (EGF) through the RF microchannels were investigated in photo-damaged skin.

Results The cumulative amounts of active ingredients through the RF microporated skin were significantly increased. Topically applied α-bisabolol after RF microporation induced rapid onset of skin whitening and significantly increased the ΔL-value of UVB-induced hyperpigmented melanin hairless mouse skin. In addition, wrinkle formation after topical application of EGF with RF microporation was significantly reduced and prevented after 12 weeks, and all parameters involving wrinkles in a replica analysis were similar to those in the negative control.

Conclusions RF microporation enhances the topical delivery of active ingredients with high molecular weight or of small hydrophilic or lipophilic molecules. Thus, this technology can effectively improve photo-induced hyperpigmentation and wrinkle formation by enhancing topical delivery of active agents.

KEY WORDS ablation · epidermal growth factor · microporation · radiofrequency · topical delivery

J. Kim • J.-H. Jang • J. H. Lee • J. K. Choi • W.-R. Park • I.-H. Bae • J. Bae • J. W. Park (✉)
Amorepacific Corporation R&D Center
314-1, Bora-dong, Giheung-gu
Yongin-si, Gyeonggi-do 446-729, South Korea
e-mail: jwpark@amorepacific.com

ABBREVIATIONS

EGF	epidermal growth factor
ER	enhancement ratio
FITC	fluoroscein isothiocyanate
MW	molecular weight
PBS	phosphate buffered saline
RF	radiofrequency
SC	stratum corneum
UVB	ultraviolet-B

INTRODUCTION

Stratum corneum (SC), the outmost dermal layer, is the barrier that protects against delivery of external molecules across the skin. Therefore, the transdermal delivery of large molecules, such as proteins or peptides, and highly water soluble molecules is remarkably restricted (1,2). Due to these limitations, technologies for the active transdermal delivery of drugs have been developed (3,4). Microporation-based drug delivery devices for the delivery of drug molecules across this biological barrier have been developed as third-generation enhancement strategies that will have a significant impact on transdermal delivery. Numerous technologies have been investigated for skin microporation by physical methods, such as microneedles (5,6), iontophoresis (6,7), ultrasound/phonophoresis or sonophoresis (8,9), high pressure gas microporation (10–12), laser or thermal ablation (13–15), electroporation (16), and radiofrequency (RF) microporation (17,18).

Microneedles consist of a plurality of microprojection arrays of different shapes, generally ranging from 100 to 1,000 μm in height, that are attached to a base support; the application of such an array can create transport pathways of micron dimension in the biological membrane and is the

most broadly used skin poration method to enhance the penetration of active ingredients for both health and skin care. However, the inherent elasticity and irregular surface of the skin remains a major challenge in the reproducibility of microneedle penetration. In addition, insertion of microneedles into any biological membrane needs sufficient strength. But, microneedles prepared by hard or brittle polymeric materials may inhibit drug delivery or facture during application. Further challenges also lie in the stability of microneedles, denaturation of macromolecular drug during fabrication and storage, and manufacturing cost. Iontophoresis is used with skin regenerative ingredients to assist skin rejuvenation treatment. But, in this method, the active ingredient solution should be charged for efficient permeation; this method is not proper for penetration of large molecular weight active ingredients such as proteins and peptides. High pressure gas microporation is a needleless injection by high pressure micro-jet injector for efficient delivery of macromolecules, including DNA, insulin, growth hormones, vaccines and other biotechnology products, and aesthetic filler. Although this type of injection can be performed with less pain than syringe injection and with cycling injection, the operating sound is quite loud and injuries can occur at the treatment site by inappropriate injection. The micro-jet injectors are being investigated with the aim of maintaining more reproducible and consistent drug delivery rates, as well as reducing the occurrence of pain. Laser and thermal microporations are also used for transdermal drug delivery and fractional treatment for skin resurfacing and rejuvenation. These methods enhance the skin permeability of active ingredients through microchannels formed by direct heat-induced damage that results in micro-explosions. However, these treatments often result in longer downtime than RF treatment and additional studies are required to demonstrate their clinical safety (19).

RF thermal ablation is a well-known technology used to destroy malignant tissue and to ablate sebaceous glands that cause acne. RF ablation is performed by a series of reactions conducting an alternating electrical current. Micropores are created by placing a microelectrode-array against the skin. The RF energy, produced by alternating electrical current at a frequency higher than 100 kHz, induces ionic vibrations between electrodes with (+) charge or (−) charge. This heats the tissues, leading to water evaporation and cell ablation and forming microchannels from the SC to outer dermis in depth. The creation of hydrophilic microchannels, which fill with interstitial fluid immediately after channel formation, can be adapted to drug delivery technology as an optional physical enhancer (17).

RF microporation technology has been used for transdermal drug delivery of macromolecules or hydrophilic agents, such as hormones, peptides, vaccines, DNA, and small interfering RNA. Recently, RF energy was also applied to acne treatment (20), body contouring (21), and skin resurfacing and rejuvenation (22,23). RFAL (Radiofrequency Assisted Liposuction) has been used for body tightening with deep region heating and soft tissue contraction (24). Insulated RF needle system has been used for acne treatment. In particular, fractional RF treatment has been widely used for skin resurfacing by removing scar and skin rejuvenation by inducing collagen formation because the treatment with RF microporation results in much less pain and a shorter downtime than fractional laser therapy (19,25).

Cosmeceuticals and dermatologists treating an aging population overexposed to the sun have increasingly focused on skin rejuvenation. Some symptoms of photo-aged skin, including wrinkles and hyperpigmentation, have been treated by various noninvasive treatments and cosmeceuticals (26). Especially, UVB exposure stimulates collagenase production by human dermal fibroblasts (HDF) and upregulates collagenase gene expression in the dermis. This subsequently induces collagen degeneration and deposition of altered elastic tissue, which are prominently observed as wrinkles and yellow discoloration of skin (27,28). Lasers and several cosmeceuticals, such as derivatives of retinol, vitamin C and topical growth factors, all of which induce collagen synthesis from HDF, have been used to treat skin texture and wrinkling (29).

In this study, we designed a RF-microchanneling device to overcome differences in skin condition, impedance and consequential variation of input energy. This design is essential for forming RF microchannels with consistent, well-controlled depths and widths. Then, we investigated the enhancing effect of RF microchannel formation on skin permeation of various active ingredients and efficacy in photo-damaged skin. The specific objectives were (i) to investigate the enhancing effect of RF microchannels on skin permeation of fluorescence-conjugated dextrans of various molecular weights as a function of RF fluence and molecular size by using the Franz diffusion cell system to find the optimum operating parameters of RF microporation, (ii) to investigate the enhancing effect of microchannels on skin permeation of active ingredients, (iii) to investigate the enhancing effect of RF microchannels on preclinical efficacy of active ingredients to improve symptoms related to UVB-induced photo-damage.

MATERIALS AND METHODS

Materials

Fluorescein isothiocyanate (FITC) dextran with an average molecular weight (MW) of 4,000, 10,000, 20,000, or 40,000; arbutin; α-bisabolol; and polyethylene glycol 400 (PEG 400)

were purchased from Sigma-Aldrich (St. Louis, MO, USA). Epidermal growth factor (EGF) was supplied by BIO-FD&C (Incheon, South Korea). Acetonitrile (chromasolv HPLC) and ethanol (EtOH, chromasolv HPLC) were purchased from Samchun Chemical (Seoul, South Korea). All chemicals were of at least analytical grade. Deionized water (resistivity > 18 MΩcm) was used to prepare all solutions.

Fractional Radiofrequency-Microchanneling Device

The RF-microporator is made of two primary components: a reusable electronic controller similar in size to an electric shaver and a disposable array that can snap onto the end of the controller. The controller can measure the impedance of skin and adjust the electrical inputs during the ablation process to send the proper power to create micro-pores. The array is made of stainless steel electrodes 1 mm in length and 250 μm in diameter with a sharpened edge. It includes 100 electrodes spaced 1.5 mm apart in a square matrix arrangement. The electrodes are designed to create micro-pores that are 50 μm wide and 70–100 μm deep. The RF-microporator is operated as follows: the array of electrodes is pressed against the test site on the skin and then the operation button is pushed. The work of the array is completed within seconds (typically less than a millisecond per burst). As programmed, each electrode receives multiple bursts of RF energy.

Excised hairless mouse skin was treated with the following conditions for *in vitro* tests: applied voltage: 300 V; RF frequency: 500 kHz; burst length: 1 ms; number of bursts: 5 or 10; applied percentage of power: 60, 80 and 100 % by maximum output.

Animal studies were performed with the following conditions: applied voltage: 300 V; RF frequency: 500 kHz; burst length: 1 ms; number of bursts: 5; applied percentage of power: 100 %.

In Vitro Skin Permeation Study

Hairless mouse skin (Han-Lim experimental animal research center, Hwaseong, South Korea) was excised carefully from the dorsal and ventral region. The skin samples were wrapped in Parafilm™ and then stored at −20 °C for a maximum period of 1 month.

The permeability of each active molecule through hairless mouse skin was measured by Franz diffusion cell system (Laboratory Glass Apparatus, Fine Science, South Korea). The diffusion area was 0.785 cm^2. The receptor phase compartment was filled with 5.5 ml of phosphate-buffered saline (PBS, pH 7.4) or PEG 400-PBS (70:30). Skin samples, either without RF treatment (control) or after RF microporation, were mounted on the receptor phase compartments with the SC facing upwards and then the donor compartments were clamped in place. Prior to addition of the test formulations to the donor compartment, the cells were allowed to equilibrate for at least 30 min and the integrity of epidermal membranes was visually inspected. After equilibrium, test formulations were placed in the donor compartments (200 μl) and the tops of the donor compartments were sealed with paraffin film to prevent sample evaporation. The receptor compartment was stirred at room temperature with a water circulating system to maintain a skin surface temperature of 32 °C throughout the experiment; 1 ml of the receptor phase was withdrawn after 1, 3, 6, 9, 12 and 24 h, and each aliquot was replaced with fresh PBS or PEG 400-PBS (70:30). The withdrawn samples were filtered through a membrane filter (0.45 μm, PVDF) and kept at 4 °C until analyzed. Experiments were performed to evaluate the effects of RF microporation, fluence, and molecular weight on cumulative skin permeation kinetics.

Data were expressed as the cumulative permeation amount per unit of skin surface area (μg/cm^2 or pg/cm^2). The fluxes (μg/cm^2·hr or pg/cm^2·hr) were calculated by linear regression interpolation of the experimental data.

Effect of Molecular Size of an Active Ingredient on Delivery Rate

The permeability of FITC dextran with a molecular weight of 4,000, 10,000, 20,000 or 40,000 through hairless mouse skin was measured as a function of RF fluence. FITC dextran solution was made at 5 mg/ml in PBS. The receptor phase compartment was filled with PBS (pH 7.4). After adding FITC dextran solution to the donor compartment, the Franz diffusion cell system was protected from light. FITC dextran samples from the skin permeation experiments were analyzed using a microplate reader equipped with a fluorescence intensity detector (Flexstation 3, Molecular Devices Inc., USA). The quantification of FITC dextran was carried out with excitation and emission wavelengths set at 490 and 520 nm, respectively.

In Vitro Transdermal Delivery of Various Active Ingredients

The permeabilities of α-bisabolol (MW 222.37), arbutin (MW 272.25) and EGF (MW 6,045) were measured through hairless mouse skin.

α-Bisabolol solution was prepared at 5 mg/ml in PEG 400-PBS (70:30). The receptor phase compartment was also filled with PEG 400-PBS (70:30). 10 μl aliquots from each sample were injected into a HPLC system equipped with a pre-packed C18 column (Phenomenex Gemini™, 10 μm, 250 × 4.6 mm). The samples were chromatographed using an isocratic mobile phase of acetic acid (1 → 1,000)-

acetonitrile (20:80) at a flow rate of 0.8 μl/min. The quantification of α-bisabolol was carried out at 210 nm.

Arbutin solution was made at 20 mg/ml in PBS and vehicle, PEG 400-EtOH (70:30). The receptor phase compartment was filled with PBS (pH 7.4). 20 μl aliquots from each sample were injected into a HPLC system equipped with a pre-packed C18 column (Phenomenex Gemini™, 5 μm, 250×4.6 mm). The quantification of arbutin was carried out at 280 nm. The samples were chromatographed using an isocratic mobile phase consisting of monopotassium phosphate buffer (10 mM)-acetonitrile (92:8) at a flow rate of 1.0 μl/min.

EGF solution was prepared at 200 ppm in PBS and vehicle, PEG 400-PBS (70:30), for use in a preclinical study. The receptor phase compartment was filled with PBS (pH 7.4). The samples from the skin permeation experiments were analyzed using a solid phase sandwich ELISA (Invitrogen, Carlsbad, CA, USA) and the quantification of EGF was carried out at 450 nm.

In Vivo Evaluation of the Efficacy of RF Microporation for Topical Delivery of α-Bisabolol and EGF

The animals were housed in cages kept at a room temperature of 23±3 °C, relative humidity of 40~60 %. Lighting was adjusted automatically to give a cycle of 12 h light and 12 h dark. Throughout the study, the animals had *ad libitum* access to laboratory diet (Purina Co., Korea) and sterilized tap water. No contaminants were present at significant levels in either diet or water. The animals were randomly assigned to UV control, test and reference groups. All animal procedures were approved by the AmorePacific Institutional Animal Care and Use Committee (IACUC).

Topical Delivery of α-Bisabolol

Thirty-two female F5 melanin hairless mice were divided into four groups (n=10): UV+vehicle, UV+RF microporation+vehicle, UV+α-bisabolol and UV+RF microporation +α-bisabolol. The back of each mouse was exposed to UVB radiation three times a week for three consecutive weeks with 300 mJ/cm^2 per exposure. The light source was a Philips TL20W/12RS K4 lamp (n=10). After the final UVB irradiation, the backs of mice were heavily pigmented. Each test material was then applied topically to the hyperpigmented area (α-bisabolol or vehicle solution, 10 μl/site, 5 mg/ml in PEG 400/EtOH=70/30) once daily for four weeks from the day after the last tanning session; RF microporation at 100 % fluence with five bursts was also applied on the back skin of the mice in the RF treatment group twice a week before treatment with the solution.

The degree of pigmentation was assessed by the light value (L-value; brightness index) measured using a chromameter (CR-300, Minolta, Tokyo, Japan). The ΔL-value was evaluated as follows: ΔL=L-value (at each day measured) - L-value (at Day 0). An increase in the ΔL-value indicates a decrease in hyperpigmentation induced by UVB.

Skin biopsies were taken immediately after *in vivo* evaluation, by a biopsy punch, and were fixed in 4 % buffered formaldehyde solution. The samples were embedded in paraffin wax, cut to a thickness of 3 μm, stained using Fontana-Masson silver.

Topical Delivery of EGF

Sixty female hairless mice (Amorepacific experimental animal center, Yongin, Korea) weighing approximately 25 g were used for the study. Hairless mice were divided into six groups (n=10); UV control (not irradiated with UV), UV+vehicle, UV+RF microporation, UV+RF microporation+vehicle, UV+EGF, and UV+RF microporation+EGF. All groups except UV control were exposed to UVB three times a week and the irradiation intensity was increased weekly by 1 MED (minimum erythema dose) up to 4 MED, and then continued at 4 MED until the 12th week. The back of each animal was irradiated three times a week at 100 mJ/cm^2 per exposure throughout the period of this study. The light source was a Philips TL20W/12RS K4 lamp (n=10). After the final UVB irradiation, the back of each hairless mouse was heavily aged. Each test material (EGF or vehicle) was applied once daily, 50 μl/mouse, 10 ppm in PEG 400-PBS (70:30) on the skin of hairless mouse from the day after 6-week UVB irradiation (Day 43) to the day of sacrifice (Day 84). RF microporation at 100 % fluence with five bursts was applied on the back skin of the mouse of RF treatment group twice a week before treatment with the solution.

The degree of aging was assessed by TEWL (transepidermal water loss), skin thickness and wrinkle formation. TEWL was frequently used to evaluate the integrity of the skin barrier using a vapormetor SW4102 (Delfin Technologies, Kuopio, Finland). Skin thickness is increased by continuous ultraviolet radiation. Viable folding skin thickness was measured by Micrometer (Absolute, Mitutoyo, Japan). Wrinkle formation was measured by replica analysis. At the end of the test, negative replicas of the dorsal skin surface were taken using a silicon-based impression material, SILFLO (Flexico, England). For ease of measurement, all replicas were cut into circular pieces with a diameter of 1 cm, and the back of each replica was processed into a flat plane using the same impression material. Light was directed at 20° angle, and images were incorporated from replica using a CCD (Model SDC-45, Samsung, Seoul, South Korea). The image of the negative replicas was observed using a wrinkle analysis system, Skin Visiometer SV600 (Courage & Khazaka, Köln, Germany). The parameters used in the assessment of the skin wrinkles were as follows: H: horizontal; R1: distance between the

highest mountain and the lowest value; R2: biggest value of those five maximum distances; R3: average of the five maximum distances; R4: smoothness depth; R5: arithmetic average roughness.

Skin biopsies were taken by a biopsy punch immediately after *in vivo* evaluation and were fixed in 10 % buffered formaldehyde solution. The samples were embedded in paraffin wax, cut to a thickness of 6 μm, stained with Masson's trichrome staining.

Statistics

All data are expressed as mean ± SD, and Student's unpaired t-test was used for comparison between groups. A value of $p<0.05$ was considered statistically significant.

RESULTS

Effect of Fluence and Molecular Weight on FITC Dextran Transport

In vitro permeation of FITC-conjugated dextran through excised skin with or without RF microporation was investigated. The values for cumulative amount of FITC dextran ($\mu g/cm^2$) in the receptor compartment as a function of time after RF treatment at various energies are given in Fig. 1.

The permeability of FITC dextran through excised hairless mouse skin without RF poration was very low but it was significantly enhanced after RF pre-treatment as a function of fluence. For these experiments the

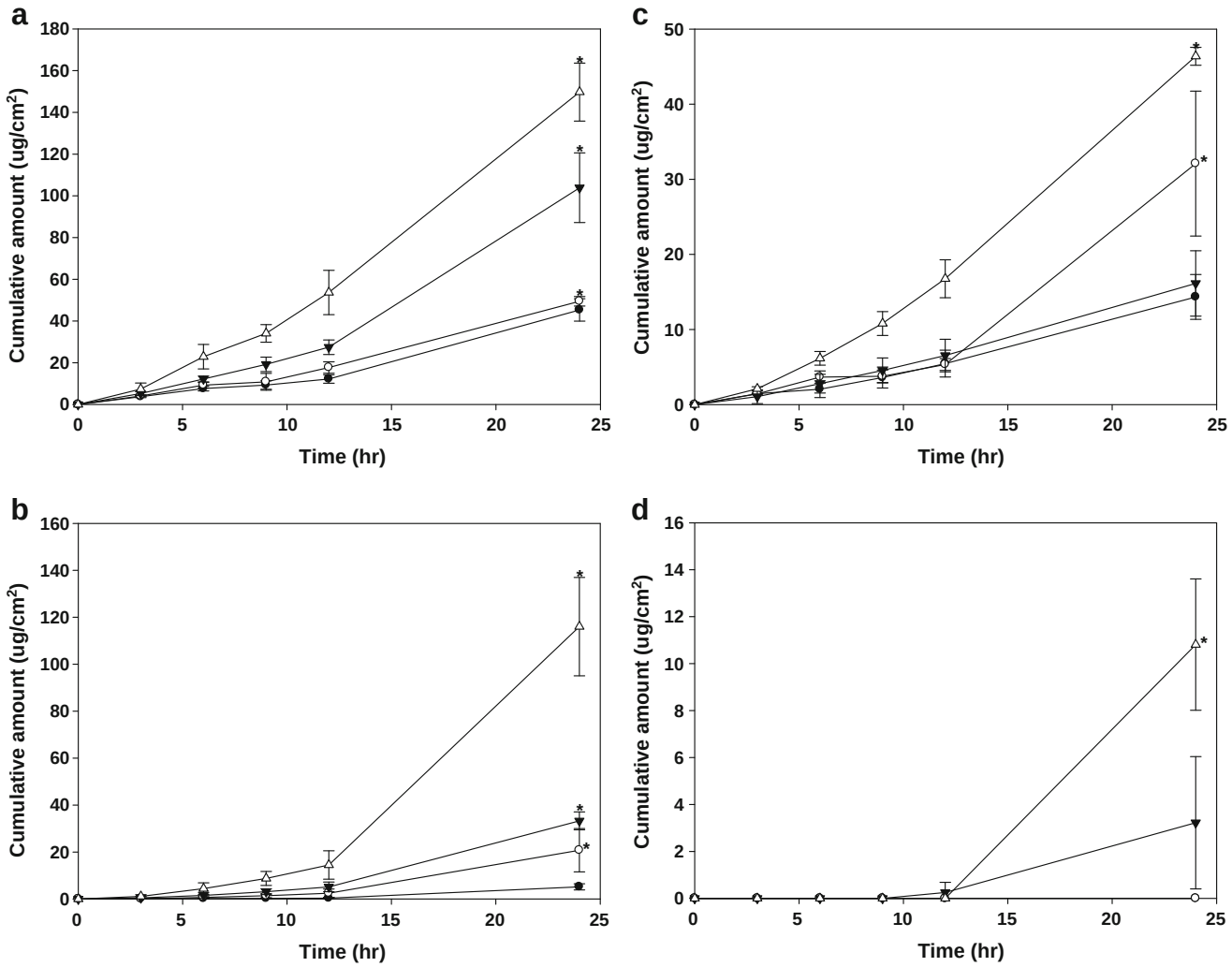

Fig. 1 *In vitro* cumulative amount-time profiles of FITC dextrans with various molecular weights after treatment with different RF microporation fluences. The permeability was measured through hairless mouse skin. Effect of RF pre-treatment was evaluated by skin permeation of FITC dextran with molecular weight of (**a**) 4,000, (**b**) 10,000, (**c**) 20,000 and (**d**) 40,000. RF pre-treatment was operated at 0 % × 10 bursts (control, ●), 60 % × 10 bursts (○), 80 % × 10 bursts (▼) and 100 % × 10 bursts (△). Data were expressed as mean ± SD ($n=6$). *$p<0.05$ compared to the cumulative permeation of untreated skin (control).

fluence held at (A) 0, (B) 60, (C) 80 and (D) 100 % of the maximum output energy. Increasing the fluence resulted in a quantitative increase in cumulative FITC dextran permeation. After 24 h, the cumulative permeations of FITC dextran with MW 4,000, 10,000, 20,000 and 40,000 were as follows: MW 4,000: 45.31±5.37, 49.45±2.28, 103.88±16.68 and 149.73±13.90 μg/cm^2; MW 10,000: 5.19±1.31, 20.77±9.25, 33.28±3.82 and 116.04±20.96 μg/cm^2; MW 20,000: 14.33±2.98, 32.09±9.65, 16.13±4.35 and 46.38±1.19 μg/cm^2; MW 40,000: 3.22±2.82 and 10.81±2.80 μg/cm^2 at 80 and 100 % fluence.

At fixed fluence (100 %), the permeability of FITC dextran with MW 4,000, 10,000, 20,000 and 40,000 was significantly decreased by increasing MW from 4,000 to 40,000 because the molecules with higher MW possessed larger molecular radii. After 24 h, the cumulative permeations were 149.73±13.90, 116.04±20.96, 46.38±1.19 and 10.81±2.80 μg/cm^2, respectively.

The flux of FITC dextran was also significantly enhanced with RF pre-treatment at 100 % fluence, as compared to that in untreated control skin. After 24 h, fluxes of 6.24±0.58, 4.84±0.87, 1.93±0.05 and 0.45±0.12 μg/cm^2·hr were obtained for FITC dextran of each molecular weight, respectively. These results were compared to fluxes of 1.89±0.22, 0.22±0.06, 0.60±0.12 and 0.00±0.00 μg/cm^2·hr after 24 h penetration through untreated skin, respectively. The RF microporation at 100 % fluence produced 3.3-, 22.0- and 3.2-fold increases in the flux of FITC dextran with molecular weight 4,000, 10,000 and 20,000, respectively, compared to the control. On the other hand, the RF pre-treatment at 80 %, the cumulative permeation of FITC dextran of each molecular weight were enhanced 2.3, 6.3 and 1.1 times than that in the untreated skin, respectively. FITC dextran with MW 40,000 penetrated only after RF pre-treatment with fluence above 80 % (Table I).

Effect of RF Microporation on Transdermal Delivery of Active Ingredients

The flux and cumulative permeation of α-bisabolol through excised hairless mouse skin with RF pre-treatment were both increased, 2.29±0.32 μg/cm^2·hr and 54.87±7.73 μg/cm^2, compared to untreated control skin, 1.64±0.36 μg/cm^2·hr and 39.32±8.63 μg/cm^2, respectively (Fig. 2a and Table II). In addition, the fluxes of arbutin and EGF, made in a test solution with PBS, through excised skin were significantly enhanced by RF pre-treatment compared to the untreated control skin (Fig. 2b, c and Table II).

After 24 h, the flux and cumulative permeation of arbutin were 31.78±5.50 μg/cm^2·hr and 762.77±132.07 μg/cm^2, respectively. Compared to the values after 24 h penetration through untreated skin, the values were 2.6 times higher than the values obtained from untreated skin (cumulative permeation: 290.48±59.22 μg/cm^2, flux: 12.10±2.47 μg/cm^2·hr). After 24 h, the flux and cumulative permeation of EGF were 129.66±12.63 pg/cm^2·hr and 3111.76±303.18 pg/cm^2, respectively. Compared to the values after 24 h penetration through untreated skin, the values were 6.8 times higher than the values obtained from untreated skin (cumulative permeation: 458.13±68.20 pg/cm^2, flux: 19.09±2.84 pg/cm^2·hr). On the other hand, the flux and cumulative amount of arbutin in test solution with vehicle were also enhanced by RF pre-treatment after 24 h, 6.93±0.52 μg/cm^2·hr and 166.90±12.57 μg/cm^2, compared to values through untreated skin, 5.18±1.35 μg/cm^2·hr and 124.32±32.33 μg/cm^2, respectively. EGF in test solution with vehicle also showed differences between RF pretreated group and untreated group in flux (23.09±2.97 and 6.04±3.20 pg/cm^2·hr) and cumulative amount (554.20±71.24 and 144.85±76.85 pg/cm^2·hr). The cumulative permeations of arbutin and EGF in test solution with vehicle were lower than those with PBS (Fig. 2c and Table II).

Table I *In Vitro* Fluxes and Enhancement Ratios (ER) of FITC Dextran Series Via Hairless Mouse Skin by Pre-treatment of Fractional RF Microporation at Different Fluences

Fluence (%)	FITC dextran 4K		FITC dextran 10K		FITC dextran 20K		FITC dextran 40K	
	Flux (μg/cm^2·hr)	ER[a]	Flux (μg/cm^2·hr)	ER	Flux (μg/cm^2·hr)	ER	Flux (μg/cm^2·hr)	ER
Control (No treat)	1.89±0.22	–[b]	0.22±0.06	–	0.60±0.12	–	0.00±0.00	–
60	2.06±0.10	1.0	0.87±0.19	4.0	1.34±0.40	2.2	0.00±0.00	–
80	4.33±0.70	2.3	1.39±0.16	6.3	0.67±0.18	1.1	0.13±0.12	–
100	6.24±0.58	3.3	4.84±0.87	22.0	1.93±0.05	3.2	0.45±0.12	–

Each value represents the mean ± SD (*N*=6)

[a] Enhancement ratio (ER) was flux of RF-pretreated group/flux of control group

[b] Not determined

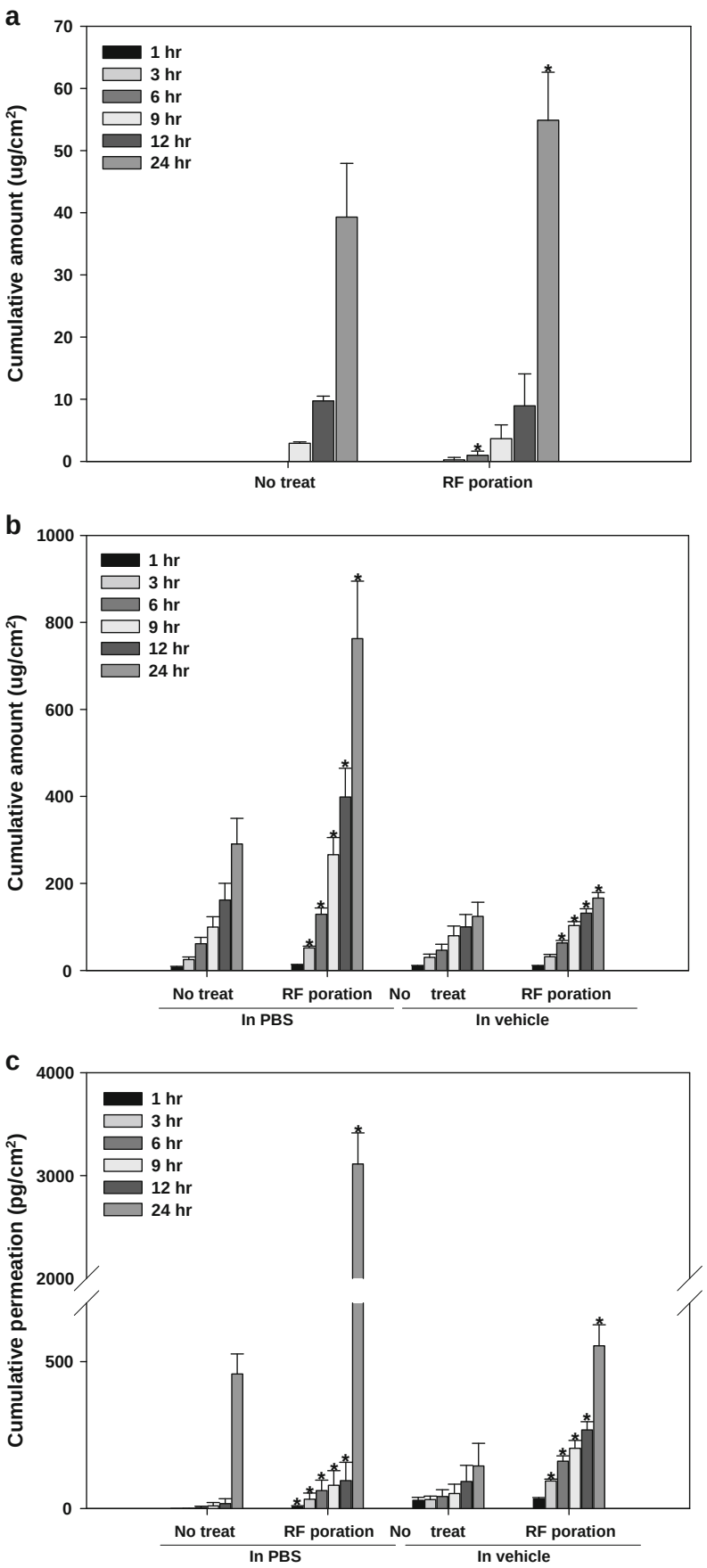

Fig. 2 Comparison of cumulative permeation through hairless mouse skin with or without fractional RF microporation at 100 % fluence with five bursts. (**a**) α-Bisabolol in PEG400-PBS (70:30). (**b**) Arbutin in PBS or PEG400-EtOH (70:30). (**c**) EGF in PBS or PEG400-PBS (70:30). Each value represents the mean ± SD ($n=6$). *$p<0.05$ compared to the cumulative permeation of untreated skin (control).

Table II *In Vitro* Flux Data of Active Ingredients Across the Skin by Passive Diffusion and RF Microporation Treatment

	Control (No treat) Flux ($\mu g/cm^2 \cdot hr$)	RF microporation Flux ($\mu g/cm^2 \cdot hr$)	ER[a]
α-Bisabolol	1.64 ± 0.36	2.29 ± 0.32	1.4
Arbutin (in PBS)	12.10 ± 2.47	31.78 ± 5.50	2.6
Arbutin (in vehicle)	5.18 ± 1.35	6.93 ± 0.52	1.3
EGF (in PBS)	19.09 ± 2.84 ($pg/cm^2 \cdot hr$)	129.66 ± 12.63 ($pg/cm^2 \cdot hr$)	6.8
EGF (in vehicle)	6.04 ± 3.20 ($pg/cm^2 \cdot hr$)	23.09 ± 2.97 ($pg/cm^2 \cdot hr$)	3.8

Each value represents the mean ± SD ($N=6$)

[a] Enhancement ratio (ER) was flux of RF-treated group/flux of control group

Effect of RF Microporation on Increasing the Active Ingredient Efficacy *In Vivo*

Figure 3 represents the depigmenting effects of RF microporation and α-bisabolol on UV-induced pigmentation at 0, 7, 14, 21, and 28 days. After 4 weeks, the ΔL-value and degree of skin whitening obtained from the dorsal skin treated with UV+RF microporation+vehicle, UV+α-bisabolol, and UV+RF microporation+α-bisabolol group (ΔL-value: 0.35 ± 1.85, 0.06 ± 1.33 and 0.68 ± 0.73, respectively; degree of skin whitening: 1.24 ± 1.30, 1.04 ± 0.94 and 1.48 ± 0.51, respectively) increased compared to those in the UV+vehicle group (ΔL-value: −1.43 ± 1.78, degree of skin whitening: 0.00 ± 1.25). α-Bisabolol with or without RF microporation reduced pigmentation from 14 days after treatment and produced a substantial reduction by 28 days. The ΔL-value obtained from the RF microporation+α-bisabolol group was significantly higher than that of the vehicle treated group and 10-fold improved compared to the group treated with α-bisabolol alone at 28 days. Moreover, the ΔL-value in the UV+RF microporation+α-bisabolol group was 0.24 ± 0.81 and showed a visible decrease in hyperpigmentation, meanwhile the ΔL-value in other groups was below zero on day 14. Interestingly, the RF microporation with vehicle also showed depigmentation effect. Therefore, the RF microporation treatment itself can cause a whitening effect on the hyperpigmentation.

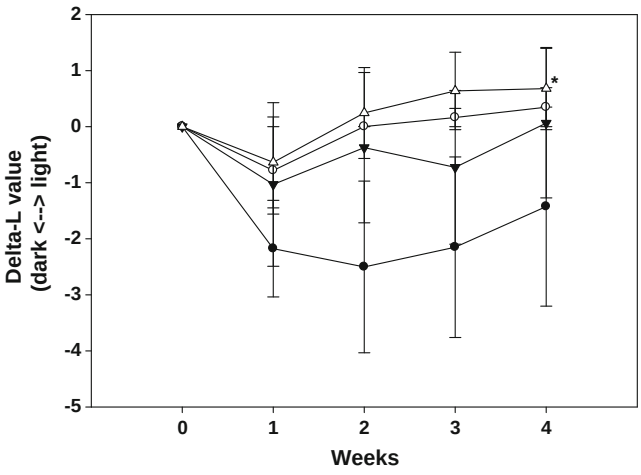

Fig. 3 The degree of pigmentation (ΔL value) after the daily topical application of the vehicle and α-bisabolol with or without twice a week RF microporation on UVB-induced hyperpigmentation in hairless mouse skin: UV+Vehicle (control, ●), UV+α-bisabolol (▼), UV+RF microporation+Vehicle (○), UV+RF microporation+α-bisabolol (△). Data were expressed as mean ± SD ($n=10$). *$p < 0.05$ *vs.* control.

Biopsy specimens were obtained after 28 days of topical application of α-bisabolol with or without RF microporation and processed for light microscopy examination of Fontana-Masson silver stains (Fig. 4). The number of melanocytes (black spots) was significantly reduced in the group treated with RF microporation and α-bisabolol. These results collectively support the synergistic effect of RF microporation and topical application of α-bisabolol to treat hyperpigmentation caused by UV irradiation or pigmented skin disorder.

During the period of UVB exposure, the mice showed fine and irregular wrinkles on their dorsal back. After 12 weeks, the levels of TEWL and skin thickness in all UV-exposed groups were significantly increased than those in the negative control group. However, the UV+RF microporation+EGF group showed lower values of TEWL and skin thickness than those of other UV-exposed groups.

The UV+RF microporation+vehicle and UV+RF microporation+EGF groups appeared to have fewer wrinkles than the UV+vehicle (control) and the UV+EGF groups after 12 weeks. In replica analysis (Fig. 5b), only RF microporation treatment also improved and prevented wrinkle formation by UVB irradiation. In addition, the parameters for the wrinkles of replicas in the UV+RF microporation+EGF group were significantly reduced compared with all other UV-exposed groups and were similar to the negative control group. However, there was no prevention or improvement effect on wrinkle formation by only topical application of EGF. Similar results were also observed from replica images (Fig. 5a). To determine the effect of topical application of EGF after RF microporation on UVB-irradiated skin, tissue sections were stained with

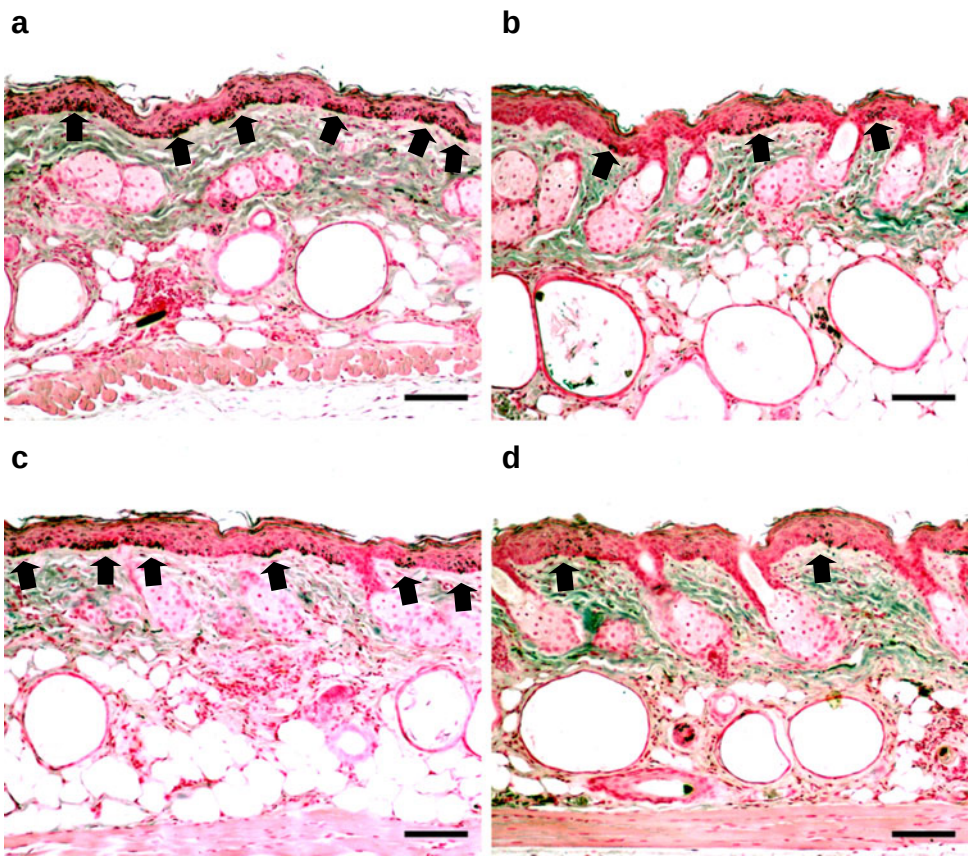

Fig. 4 Biopsy specimens from the treatment site after 28 days of topical application were processed for light microscopy examination of Fontana-Masson silver stains. Black spots were melanocytes and the number of melanocytes was significantly reduced in the groups treated with RF microporation. (**a**) UV+vehicle (control), (**b**) UV+RF microporation+vehicle, (**c**) UV+α-bisabolol, and (**d**) UV+RF microporation+α-bisabolol. Arrows on the figure indicate melanocyte cell bodies. Scale bars are 100 μm.

Masson's trichrome and then visualized under a microscope. The dermal thickness was significantly increased and an inflammatory reaction was also observed in the UV+vehicle (control) and UV+EGF groups. In contrast, the UV+RF microporation and UV+RF microporation +EGF groups showed similar histology compared with the negative control group in terms of extracellular matrix components and morphological changes. In addition, the RF microporation with or without EGF treatment showed well oriented collagen fibers and collagen fiber density was similar to the density of the normal control group, while the UVB damaged skin treated only with vehicle or EGF solution showed irregular and entangled collagen fibers and its density was significantly increased (Fig. 6).

DISCUSSION

The first objective of this study was to investigate the enhancing effect of RF microchannels on skin permeation of fluorescence-conjugated dextrans with various molecular weights as a function of RF fluence and molecular size by using the Franz diffusion cell system to find the optimum operating parameters of RF microporation. The RF microporation that removed the SC and outer layer of epidermis significantly increased fluorescence-conjugated dextrans delivery. After 24 h, the cumulative permeation of FITC dextran with MW 10,000 at 100 % of the maximum fluence was 5.6 times higher than that of at 60 % of the maximum fluence. Therefore, the permeation was highly influenced by RF fluence, implying that higher fluence made deeper and regular microchannels through the SC and epidermis and might lead to more significant changes in skin structure (30). However, the enhancement of permeation by RF fluence was not proportional to the MW. At a fixed RF fluence, the molecules with a larger molecular size (FITC dextran 10,000) generally exhibited greater enhancement of flux compared to the smaller molecules (FITC dextran 4,000). But, the enhancement of flux by microchannel formation through the diffusional barrier was decreased as the molecular weight increased above 20,000. This might be attributed to a decrease in diffusivity through the microchannels due to its larger size (31).

The second objective of this study was to determine if the RF microporation could be used to deliver active ingredients for skin therapeutic uses. From the *in vitro* tests, we found that, after 24 h, the cumulative amounts of α-bisabolol, arbutin and EGF through the RF microporated skin were increased 1.4, 2.6 and 6.8-fold over those through the control skin. However, upon comparison of the

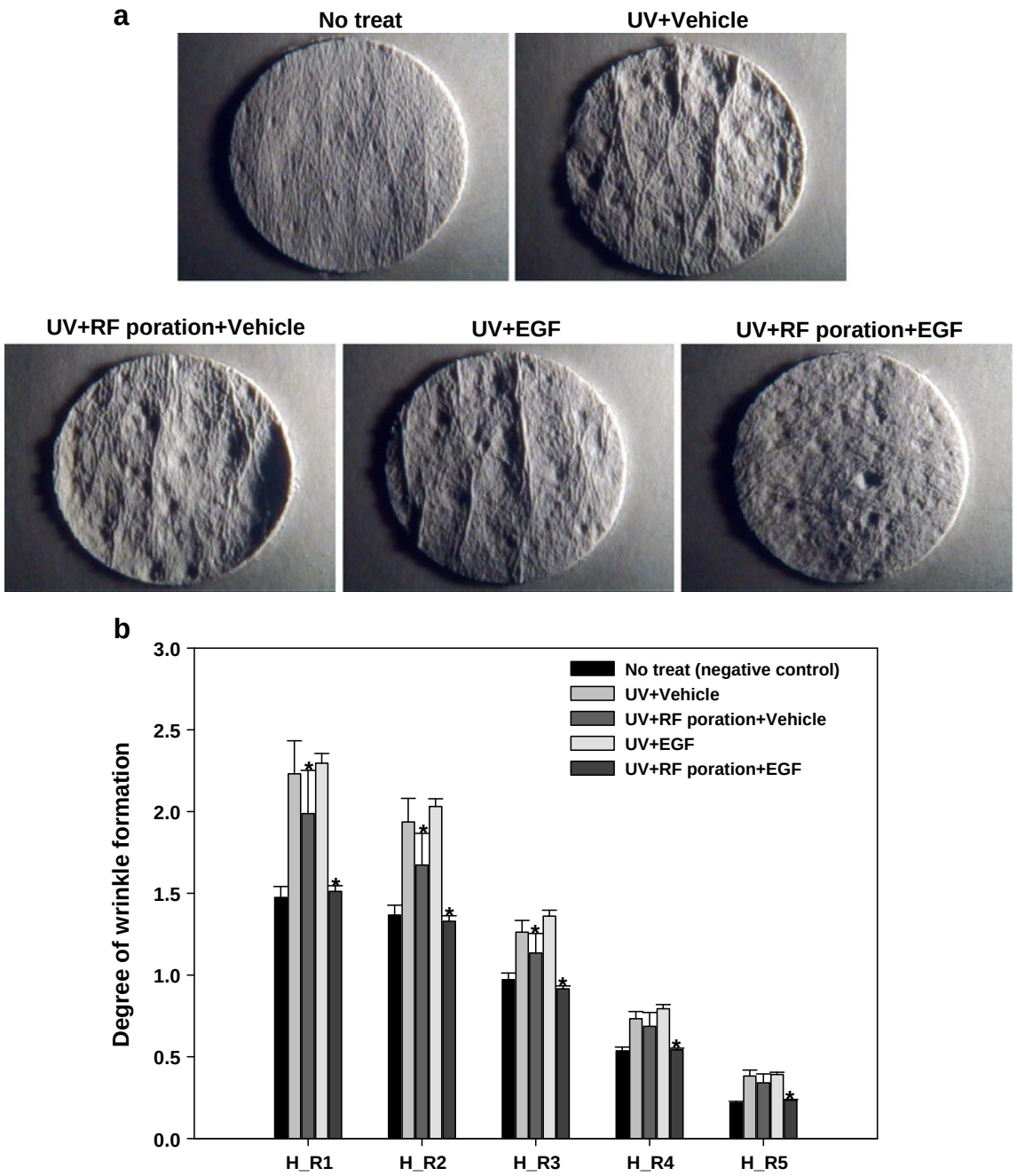

Fig. 5 Evaluation of anti-aging effect of topical application of EGF with RF microporation pre-treatment on UVB-damaged skin. (**a**) Photographs of UVB-exposed dorsal skin replicas: negative control, UV+Vehicle, UV+RF microporation+Vehicle UV+EGF, and UV+RF microporation+EGF. (**b**) Improved parameters for wrinkles. To assess skin wrinkles quantitatively, a visiometer was used to analyze replica surfaces: H: horizontal; R1: distance between the highest mountain and the lowest value; R2: biggest value of those five maximum distances; R3: average of the five maximum distances; R4: smoothness depth; R5: arithmetic average roughness. Ten animals were used in each group, mean ± SD. * $p < 0.05$ *vs.* UV+Vehicle.

cumulative permeations and fluxes of arbutin and α-bisabolol through excised animal skin *in vitro*, arbutin was 3 to 14 times more permeable through the RF pre-treated skin than α-bisabolol. Although the molecular weight of α-bisabolol is similar to that of arbutin (272 *vs.* 222), there are significant differences in partition coefficients (Log P) between α-bisabolol and arbutin (−1.49 *vs.* 5.07). Therefore, α-bisabolol acts as a lipophilic component and can easily partition into the SC. The ablation of the SC layer can reduce the inherent barrier properties of SC and thus increase the skin permeation of α-bisabolol; however, the partition of lipophilic molecules into the SC may be retarded because of the limited area of the SC after ablation. Therefore, the increased permeation into the skin due to

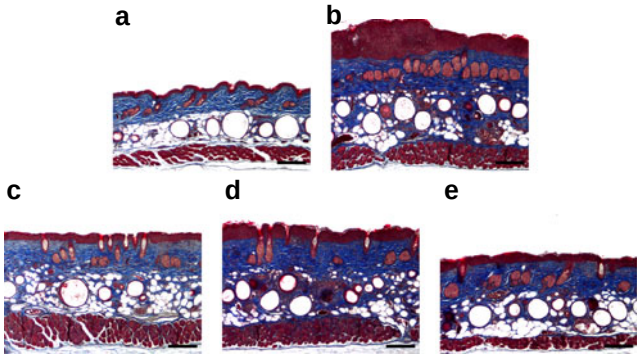

Fig. 6 Histological analysis of skin from UVB-exposed hairless mouse stained with Masson's trichrome. The dermal thickness and irregular and entangled collagen fiber density were significantly increased in the UVB-damaged skin treated only with vehicle or EGF. (**a**) Negative control, (**b**) UV+Vehicle, (**c**) UV+RF microporation+Vehicle, (**d**) UV+EGF, and (**e**) UV+RF microporation+\EGF. Scale bars are 100 μm.

skin structural ablation may be partly offset by a reduction in the partition coefficient (32). In addition, the enhancement of skin permeation thorough the microchannels was dependent on the hydrophilic properties and molecular size of the active ingredients, as well as on the vehicle. After 24 h, the fluxes of arbutin and EGF in test solution with vehicle were 4.6 and 5.6 times lower than those with PBS. This result may indicate that the viscous PEG 400 made partitioning through the epidermis layer difficult and this phenomenon was noticeable for EGF with its larger molecular weight (33).

The third objective, the ultimate purpose of this study, is to investigate the enhancing effect of RF microchannels on preclinical efficacy of active ingredients to improve symptoms related to UVB-induced photo-damage; hyperpigmentation and photo-aging.

Hyperpigmentation is the darkening of an area of skin caused by increased melanin. Hyperpigmentation may be caused by various inflammatory skin disorders, such as sun damage, inflammation or other skin injuries. Epidermal and dermal hyperpigmentation may depend on either increased numbers of melanocytes or increased melanogenic enzyme activities. Abnormal release of α-MSH (alpha-melanocyte stimulating hormone), ultraviolet light, chronic inflammation, and rubbing of the skin are triggering factors for these disorders. α-MSH induces cAMP production and tyrosinase gene expression through the activation of MITF (Microphtalmia-associated transcription factor) gene expression. These molecules are involved in the signaling pathway and promote melanin synthesis. α-Bisabolol, a sesquiterpene alcohol, possesses depigmenting activity and inhibits melanogenesis by lowering intracellular α-MSH-induced cAMP production, operating upstream of the cAMP production step; it also inhibits the production of MITF protein and the downstream molecules, tyrosinase and TRP 1 (Tyrosinase related protein 1) (34,35). In this study, we found that topical administration of α-bisabolol can be enhanced by RF microchannel formation. In addition, the RF pre-treatment itself also showed a whitening effect by skin regeneration through activation of the wound healing process, such as collagen remodeling, because the surrounding tissue of the zone of ablation acts as a reservoir of stem cells, growth factors, and inflammatory cells that quickly respond to the thermal injury and facilitate rapid recovery. Therefore, topical delivery of depigmenting agent to reduce hyperpigmentation can provide an improved whitening effect and rapid onset by combined treatment with RF microporation.

Photo-aging is a complex process with pathologic similarities to skin wounding and healing; indeed, several studies on the pathophysiology of photo-aging have found correlations with certain aspects of wound healing (36). Dermal fibroblasts, which interact with keratinocytes, fat cells and mast cells, play key roles in these processes. They are also the source of extracellular matrix proteins, glycoproteins, adhesive molecules and various cytokines (37). As they supply these molecules and support cell-to-cell interactions, skin fibroblasts contribute to the fibroblast–keratinocyte–endothelium complex that accelerates wound repair and maintains the skin integrity and youthfulness. Conventional treatments of skin aging, such as laser and topical regimens, are mostly based on increasing ECM synthesis via fibroblast activation. Collagen remodeling is the most significant skin rejuvenation process for photo-damage, and the dermal fibroblast is the most important cell in that process. A variety of growth factors including TGF (transforming growth factor), IGF (insulin-like growth factor), PDGF (platelet-derived growth factor), EGF, and FGF (fibroblast growth factor) stimulate collagen synthesis by fibroblasts (29). Among them, EGF is a potent mitogen that can induce wound healing, hair growth, skin rejuvenation, etc. EGF binds EGFR (epidermal growth factor receptor) on the cell surface with high affinity, and a subclass of high-affinity EGF receptor (EGFR) contributes to activation of the EGFR signal transduction cascade. Binding of EGF to the receptor causes dimerization of EGFRs and induces the phosphorylation of tyrosine residues on the receptor, which then leads to activation of extracellular signal-regulated kinase (ERK), inducing DNA synthesis and cell proliferation (38). Therefore, EGF has been used as an important component to improve symptoms related to photo-aging and wound healing. However, topically applied EGF cannot be absorbed though SC because of its high molecular weight and hydrophilicity. Topical administration of EGF did not improve or prevent photo-damage to the skin. In contrast, EGF treatment after RF microporation showed synergistic effects in the treatment of

photo-damaged skin due to the enhanced skin permeation of EGF and its own resurfacing effect via collagen shrinkage and dermal collagen remodeling.

CONCLUSIONS

The results of this study showed that the radiofrequency microporation technology successfully enhanced the permeation of active substances, even those with high molecular weights, by microchannel formation through the SC and epidermis layer. Topical delivery of active molecules after RF pre-treatment was also influenced and controlled by molecular size, lipophilicity, vehicle formulation, and RF fluence. In the *in vivo* studies, RF microporation significantly improved the depigmentation and anti-wrinkle efficacy of topically applied active agents to the photo-damaged skin due to enhancement of permeation and its own characteristics in modulating skin histology, such as through collagen remodeling. Therefore, considering the clinical efficacy and synergistic effect with active ingredients, RF microporation technology has great promise for application in medical and cosmetic dermatology, especially in treating photo-damaged skin.

REFERENCES

1. Naik A, Kali YN, Guy RH. Transdermal drug delivery: Overcoming the skin's barrier function. Pharm Sci Technol Today. 2000;3 (9):318–26.
2. Elias PM, Choi EH. Interactions among stratum corneum defensive functions. Exp Dermatol. 2005;14(10):719–26.
3. Prausnitz MR, Mitragotri S, Langer R. Current status and future potential of transdermal drug delivery. Nat Rev Drug Discov. 2004;3:115–24.
4. Singh TR, Garland MJ, Cassidy CM, Mijalska K, Demir YK, Abdelghany S, *et al.* Microporation techniques for enhanced delivery of therapeutic agents. Recent Pat Drug Deliv Formul. 2010;4(1):1–17.
5. Donnelly RF, Morrow DIJ, McCarron PA, Woolfson AD, Morrissey A, Juzenas P, *et al.* Microneedle-mediated intradermal delivery of 5-aminolevulinic acid: potential for enhanced topical photodynamic therapy. J Control Release. 2008;129(3):154–62.
6. Wu XM, Todo H, Sugibayashi K. Enhancement of skin permeation of high molecular compounds by a combination of microneedle pretreatment and iontophoresis. J Control Release. 2007;118(2):189–95.
7. Dubey S, Kalia YN. Non-invasive iontophoretic delivery of enzymatically active ribonuclease A (13.6 kDa) across intact porcine and human skins. J Control Release. 2010;145(3):203–9.
8. Polat BE, Hart D, Langer R, Blankschtein D. Ultrasound-mediated transdermal drug delivery: mechanisms, scope, and emerging trends. J Control Release. 2011;152(3):330–48.
9. Machet L, Boucaud A. Phonophoresis: efficiency, mechanisms and skin tolerance. Int J Pharm. 2002;243(1–2):1–15.
10. Baxter J, Mitragotri S. Jet-induced skin puncture and its impact on needle-free jet injections: experimental studies and a predictive model. J Control Release. 2005;106(3):361–73.
11. Stachowiak JC, Li TH, Arora A, Mitragotri S, Fletcher DA. Dynamic control of needle-free jet injection. J Control Release. 2009;135(2):104–12.
12. Han TH, Hah JM, Yoh JJ. Drug injection into fat tissue with a laser based microjet injector. J Appl Phys. 2011;109(9):093105.
13. Bachhav YG, Summer S, Heinrich A, Bragagna T, Böhler C, Kalia YN. Effect of controlled laser microporation on drug transport kinetics into and across the skin. J Control Release. 2010;146(1):31–6.
14. Lee WR, Shen SC, Pai MH, Yang HH, Yuan CY, Fang JY. Fractional laser as a tool to enhance the skin permeation of 5-aminolevulinic acid with minimal skin disruption: a comparision with conventional erbium:YAG laser. J Control Release. 2010;145(2):124–33.
15. Lee JW, Gadiraju P, Park JH, Allen MG, Prausnitz MR. Microsecond thermal ablation of skin for transdermal drug delivery. J Control Release. 2011;154(1):58–68.
16. Wong TW, Chen CH, Huang CC, Lin CD, Hui SW. Painless electroporation with a new needle-free microelectrode array to enhance transdermal drug delivery. J Control Release. 2006;110 (3):557–65.
17. Sintov AC, Krymberk L, Daniel D, Hannan T, Sohn Z, Levin G. Radiofrequency-driven skin microchanneling as a new way for electrically assisted transdermal delivery of hydrophilic drugs. J Control Release. 2003;89(2):311–20.
18. Levin G, Gershonowitz A, Sacks H, Stern M, Sherman A, Rudaev S, *et al.* Transdermal delivery of human growth hormone through RF-microchnnels. Pharm Res. 2005;22(4):550–5.
19. Moetaz E, Tarek SE, Walid M, Osama M, Donna B, My GM, *et al.* Radiofrequency facial rejuvenation: Evidence-based effect. J Am Acad Dermatol. 2011;64(3):524–35.
20. Dierickx CC. Lasers, light and radiofrequency for treatment of acne. Med Laser Appl. 2004;19(4):196–204.
21. Mulholland RS, Paul MD, Chalfoun C. Noninvasive body contouring with radiofrequency, ultrasound, cryolipolysis, and low-level laser therapy. Clin Plast Surg. 2011;38(3):503–20.
22. Sadick N. Bipolar radiofrequency for facial rejuvenation. Facial Plast Surg Clin North Am. 2007;15(2):161–7.
23. El-Domyati M, El-Ammawi TS, Medhat W, Moawad O, Brennan D, Mahoney MG, *et al.* Radiofreqency facial rejuvenation: Evidence-based effect. J Am Acad Dermatol. 2011;64 (3):524–35.
24. Berry MG, Davies D. Liposuction: A review of principles and techniques. J Plast Reconstr Aesthet Surg. 2011;64(8):985–92.
25. George H, Amy FT, Susannah LC, Stephen RM. Skin rejuvenation and wrinkle reduction using a fractional radiofrequency system. J Drugs Dermatol. 2009;8(3):259–65.
26. Rabe JH, Mamelak AJ, McElgunn PJS, Morison WL, Sauder DN. Photoaging: Mechanisms and repair. J Am Acad Dermatol. 2006;55(1):1–19.
27. Talwar HS, Griffiths CE, Fisher GJ, Hamilton TA, Voorhees JJ. Reduced type I and type III procollagens in photodamaged adult human skin. J Invest Dermatol. 1995;105:285–90.
28. Bernstein EF, Chen YQ, Kopp JB, Fisher L, Brown DB, Hahn PJ, *et al.* Long-term sun exposure alters the collagen of the papillary dermis. Comparison of sun-protected and photoaged skin by northern analysis, immunohistochemical staining, and confocal laser scanning microscopy. J Am Acad Dermatol. 1996;34 (2):209–18.
29. Fitzpatrick RE, Rostan EF. Reversal of photodamage with topical growth factors: a pilot study. J Cosmet Laser Ther. 2003;5(1):25–34.
30. Vavbever R, Pliquett UF, Preat V, Weaver JC. Comparison of the effects of short, high-voltage and long medium voltage pulses on skin electrical and transport properties. J Control Release. 1999;60 (1):35–47.

31. Lombry C, Dujardin N, Preat V. Transdermal delivery of macromolecules using skin electroporation. Pharm Res. 2000;17(1):32–7.
32. Sung KC, Fang JY, Wang JJ, Hu OY. Transdermal delivery of nalbuphine and its prodrugs by electroporation. Eur J Pharm Sci. 2003;18(1):63–70.
33. Vanbever R, Preat V. Factors affecting transdermal delivery of metoprolol by electroporation. Bioelectrochem Bioenerg. 1995;38 (1):223–8.
34. Kim S, Lee J, Jung E, Huh S, Park JO, Lee JW, *et al.* Mechanisms of depigmentation by [alpha]-bisabolol. J Dermatol Sci. 2008;52 (3):219–22.
35. Nishioka E, Funasaka Y, Kondoh H, Chakraborty AK, Mishima Y, Ichihashi M. Expression of tyrosinase, TRP-1 and TRP-2 in ultraviolet-irradiated human melanomas and melanocytes: TRP-2 protects melanoma cells from ultraviolet B induced apoptosis. Melanoma Res. 1999;9(5):433–43.
36. Watson RE, Griffiths CE. Photogenic aspects of cutaneous photoaging. J Cosmet Dermatol. 2005;4(4):230–6.
37. Le Pillouer-Prost A. Fibroblast: what's new in cellular biology? J Cosmet Laser Ther. 2003;5(3–4):232–8.
38. Kim WS, Park BS, Park SG, Kim HK, Sung JH. Antiwrinkle effect of adipose-derived stem cell: activation of dermal fibroblast by secretory factors. J Dermatol Sci. 2009;53(2):96–102.